

# Generative Human-Object Interaction Detection via Differentiable Cognitive Steering of Multi-modal LLMs

Zhaolin Cai<sup>1</sup>, Huiyu Duan<sup>1†</sup>, Zitong Xu<sup>1</sup>, Fan Li<sup>2</sup>, Zhi Liu<sup>3</sup>,  
Jing Liu<sup>4</sup>, Wei Shen<sup>3</sup>, Xiongkuo Min<sup>1†</sup> Guangtao Zhai<sup>1†</sup>

<sup>1</sup>Institute of Image Communication and Network Engineering, Shanghai Jiao Tong University

<sup>2</sup>Xi'an Jiao Tong University, <sup>3</sup>Shandong University, <sup>4</sup>Tianjin University

{huiyuduan, xuzitong, zhangkaiwei, qiang.hu, minxiongkuo, zhaiguangtao}@sjtu.edu.cn

## Abstract

*Human-object interaction (HOI) detection aims to localize human-object pairs and the interactions between them. Existing methods operate under a closed-world assumption, treating the task as a classification problem over a small, predefined verb set, which struggles to generalize to the long-tail of unseen or ambiguous interactions in the wild. While recent multi-modal large language models (MLLMs) possess the rich world knowledge required for open-vocabulary understanding, they remain decoupled from existing HOI detectors since fine-tuning them is computationally prohibitive. To address these constraints, we propose **GRASP-HOI**, a novel Generative Reasoning And Steerable Perception framework that reformulates HOI detection from the closed-set classification task to the open-vocabulary generation problem. To bridge the vision and cognitive, we first extract hybrid interaction representations, then design a lightweight learnable cognitive steering conduit (CSC) module to inject the fine-grained visual evidence into a frozen MLLM for effective reasoning. To address the supervision mismatch between classification-based HOI datasets and open-vocabulary generative models, we introduce a hybrid guidance strategy that coupling the language modeling loss and auxiliary classification loss, enabling discriminative grounding without sacrificing generative flexibility. Experiments demonstrate state-of-the-art closed-set performance and strong zero-shot generalization, achieving a unified paradigm that seamlessly bridges discriminative perception and generative reasoning for open-world HOI detection.*

## 1. Introduction

Human-object interaction (HOI) detection aims to localize human-object pairs and identify interactions connecting them, which is essential for applications in

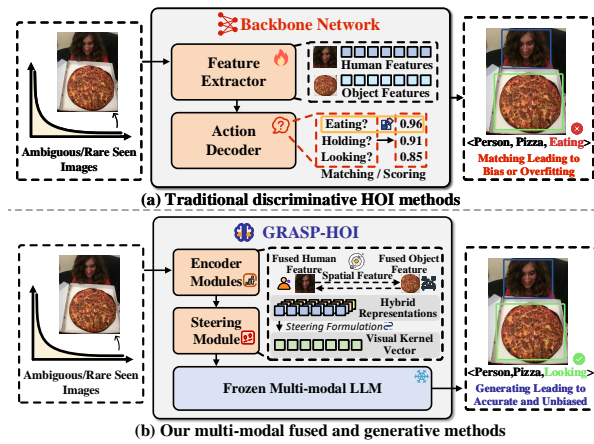


Figure 1. An overview of the traditional discriminative matching method and the proposed generative reasoning paradigm for HOI detection. (a) Traditional methods classify each detected human-object pair via classification or matching, limiting to frequent labels. (b) GRASP-HOI fuses multi-source features to steer a frozen MLLM, generating context-aware interactions beyond closed-set.

cluding visual understanding [14, 45], scene graph generation [21, 55] and embodied artificial intelligence [29, 31] etc. While significant progresses have been made in traditional HOI detection [11], these advancements are largely anchored to a closed-world classification paradigm. This dominant approach, which trains models with classification heads to select verbs from a small predefined vocabulary, has achieved remarkable performance on existing widely used datasets [5, 8, 51]. However, the reliance on a fixed label set constitutes a fundamental paradigmatic bottleneck, limiting their generalization capabilities on unseen, compositional, or ambiguous interactions in real-world scenarios.

Recent advances in large language models (LLMs) [1, 36, 48] and multimodal large language models (MLLMs) [3, 24, 61] have demonstrated impressive

open-world reasoning capabilities. These models possess extensive world knowledge and linguistic abstraction that enable fine-grained understanding beyond fixed label spaces. However, leveraging such models for HOI remains unaddressed. Frozen MLLMs are generative in nature yet inaccurate and uncontrollable, while fine-tuning MLLMs on specific HOI datasets can lead better performance but requires substantial computational resources and even more risks catastrophic forgetting, degrading the world knowledge we seek to leverage [27, 59]. On the other hand, existing HOI detectors are highly discriminative but semantically rigid, unable to adapt beyond closed-set verb semantics [4]. This exposes a fundamental paradigm gap, *i.e.*, current systems either detect without reasoning or reason without grounding.

Several attempts have sought to extend HOI detection toward open-vocabulary recognition by coupling visual encoders with pretrained text models [32, 43, 50]. While these approaches enlarge the verb space through textual similarity or compositional prompts, they remain passive matchers rather than active generators, simply transferring the label bottleneck from visual categories to textual embeddings. Consequently, they still fail to express new interactions that require contextual or causal reasoning, such as catching a falling book or holding a phone to illuminate. We argue that this failure stems from their reliance on shallow correlation alignment rather a genuine comprehension with the deep causal and functional reasoning.

More recently, some studies have explored using LLMs or MLLMs as captioning assistants for detected entities [4, 12, 26]. Although these efforts reflect a growing interest in generative understanding, they remain passive utilization of large models, treating them as external captioners or auxiliary classifiers detached from the visual understanding and detecting process [4, 19, 50]. Such designs fail to unlock the interactive potential of MLLMs, as they lack a mechanism to proactively utilize and steer them for human-object interaction detection. This leaves a critical blank spot, *i.e.*, the absence of a framework that can actively utilize a frozen MLLM visual reasoning and generating results.

To address above constraints, we propose **GRASP-HOI**, (Generative Reasoning And Steerable Perception for HOI detection), a framework that transforms HOI detection from passive matching to the active generative reasoning paradigm. Instead of tuning or prompting a large multimodal model, GRASP-HOI establishes a differentiable cognitive and knowledge interface between vision and language, which allows structured visual features to dynamically steer a frozen MLLM toward task-aligned reasoning. Specifically, GRASP-HOI first extracts hybrid interaction representations, then learns to

convert interaction-centric visual representations into an internal cognitive state that modulates the MLLM’s generation trajectory while preserving its pretrained world knowledge. Through this synergy, with the help of language loss and classification loss, perception constrains cognition with pixel-level grounding, whereas cognition enriches perception with causal and functional semantics. The resulting system unifies the discriminative precision of classical detectors with the semantic generality of large generative models, enabling both robust closed-set performance and flexible open-vocabulary reasoning. By turning passive exploitation of MLLMs into active, trainable cognitive collaboration, GRASP-HOI advances a paradigm shift from detection-by-classification to reasoning-by-generation, bridging visual grounding and high-level conceptual understanding within a single, coherent framework. Our contributions are as follows:

- We introduce GRASP-HOI, a novel framework that reframes HOI detection as preceptual generation by steering a frozen MLLM with visual evidence, shifting from the closed-set classification to open world generation.
- We design the cognitive steering conduit (CSC), a novel hybrid guidance mechanism that establishes controllable generative reasoning between structured visual representations and a frozen MLLM.
- We develop a hybrid generative objective that couples language modeling, cross-modal alignment, and commonsense constraints with detection losses, ensuring generation grounded and evaluable.
- We conduct comprehensive experiments on HICO-DET and V-COCO, demonstrating state-of-the-art performance in standard benchmarks and substantial gains under zero-shot and open-vocabulary settings.

## 2. Related Work

### 2.1. Traditional HOI detection

Traditional HOI detectors typically follow either a two-stage or one-stage paradigm [11]. Two-stage methods first rely on object detector to localize humans and objects, and then construct interaction representations through multi-stream feature fusion, including appearance, spatial configuration, human pose, or other cues [25, 40, 56]. To enhance contextual reasoning, several works further integrate graph neural networks to propagate relational information among detected entities [33, 34]. In contrast, one-stage approaches unify detection and interaction recognition within a transformer-based decoder, such as DETR-style architectures, achieving greater efficiency and global context awareness [13, 28, 52]. Despite these advances, both paradigms treat interactions as classification over a fixed verb set, thus inherently constrained by closed-

world semantics. This limitation has motivated growing interest in open-vocabulary HOI detection.

## 2.2. Open-vocabulary HOI Detection

To overcome the restricted label space, recent studies explore open-vocabulary HOI recognition through three primary directions. The first category adopts compositional learning to generalize unseen  $\langle$ human, verb, object $\rangle$  combinations [46, 50]; the second emphasizes large-scale pretraining by exploiting external datasets or pseudo-labeled data to broaden the verb-object coverage [22, 51, 60]; and the third incorporates vision-language models (VLMs) for cross-modal alignment [32, 39, 42]. Among the latter, some distill knowledge from VLMs into HOI detectors during training, while others directly fuse VLM features or textual embeddings to improve interaction recognition [26, 53]. Although these methods expand the vocabulary and improve zero-shot matching, they still operate as passive matchers, relying on static text embeddings or similarity ranking rather than genuine generative reasoning. Consequently, they cannot synthesize novel or context-dependent interactions beyond predefined textual priors, calling for more active integration of foundational generative models.

## 2.3. Foundational Model based HOI Detection

The emergence of large language models (LLMs) [38, 47] and multimodal large language models (MLLMs) [2, 58, 61] has brought unprecedented capabilities in open-world reasoning and linguistic abstraction. Several recent works leverage such models via captioning pipelines or feature adapters to enhance interaction understanding [12]. Representative frameworks demonstrate that foundational models can be guided for visual reasoning with lightweight adapters or prompts [15, 17]. However, when applied to HOI detection, these methods remain non-differentiable or weakly coupled, lacking fine-grained visual grounding and controllable supervision. Most current systems still treat MLLMs as auxiliary captioners or feature extractors rather than actively co-reasoning with structured detectors. In contrast, our approach introduces a trainable, differentiable interface that enables active cognitive alignment between structured HOI perception and a frozen MLLM’s generative reasoning process, bridging the long-standing gap between discriminative detection and open-world understanding.

## 3. Method

GRASP-HOI introduces a novel framework that re-frames human-object interaction (HOI) detection as learnable generative process via the frozen multimodal

large language model (MLLM). As shown in Figure 2, we first construct the hybrid interaction representation that aggregates entity-level and pair-level visual evidence and use salience adjudication transformer with orchestration gate to organizes multi-source visual evidence into candidate-wise tokens. Then we perform cognitive steering process to formulate the representation into a compact evidence vector and transduces it into a visual kernel that conditions the frozen MLLM to generate potential interactions.

### 3.1. Problem Formulation

Given an image  $I$ , Human-Object Interaction (HOI) detection aims to predict a set of visually grounded triplets  $\langle b_h, v, b_o \rangle$ , where  $b_h, b_o \in \mathbb{R}^4$  denote the bounding boxes of human and object, and  $v \in \mathcal{V}$  is a verb from the verb set  $\mathcal{V}$ . We build on top of an off-the-shelf detector that provides human and object detections; these detections serve as anchors to form candidate human-object pairs. GRASP-HOI performs candidate-conditioned interaction reasoning by constructing candidate-level visual evidence and using a frozen multimodal large language model (MLLM) to generate verb predictions in a candidate-specific manner.

### 3.2. Hybrid Interaction Representation

The initial step of our framework is to construct a hybrid interaction representation with multi-source low-level visual signals. These representations are processed and provide rich substrate for cognitive steering.

**Entity-level Representations.** For each detected entity  $x$  (human or object), we form a canonical entity evidence by combining two complementary tokens including the instance token  $z_x$  from a query-based detector and the appearance token  $a_x$  obtained via RoI pooling from a vision backbone. The instance tokens encode detection-aligned semantics and localization (*what* & *where*) while the appearance tokens contribute fine-grained visual cues that are robust under distribution shift. We first project tokens to a unified dimension and then fuse them with a shallow MLP:

$$f_x = \text{MLP}_{\text{fuse}} \left( [\phi_{\text{inst}}(z_x) \parallel \phi_{\text{app}}(a_x)] \right) \in \mathbb{R}^{d_e}, \quad (1)$$

where  $\phi_{\text{inst}}(\cdot)$  and  $\phi_{\text{app}}(\cdot)$  are small projection MLPs and  $[\cdot \parallel \cdot]$  denotes concatenation. The resulting  $f_x$  is a detection-grounded, appearance-enriched evidence carrier that will be combined with pairwise geometry to construct candidate tokens for subsequent adjudication.

**Pair-Level Geometric Representations.** For a candidate pair  $k$  with boxes  $(b_h^k, b_o^k)$ , we encode geometry as

$$g_k = \phi_g(\mathcal{G}(b_h^k, b_o^k)) \in \mathbb{R}^{d_g}, \quad (2)$$

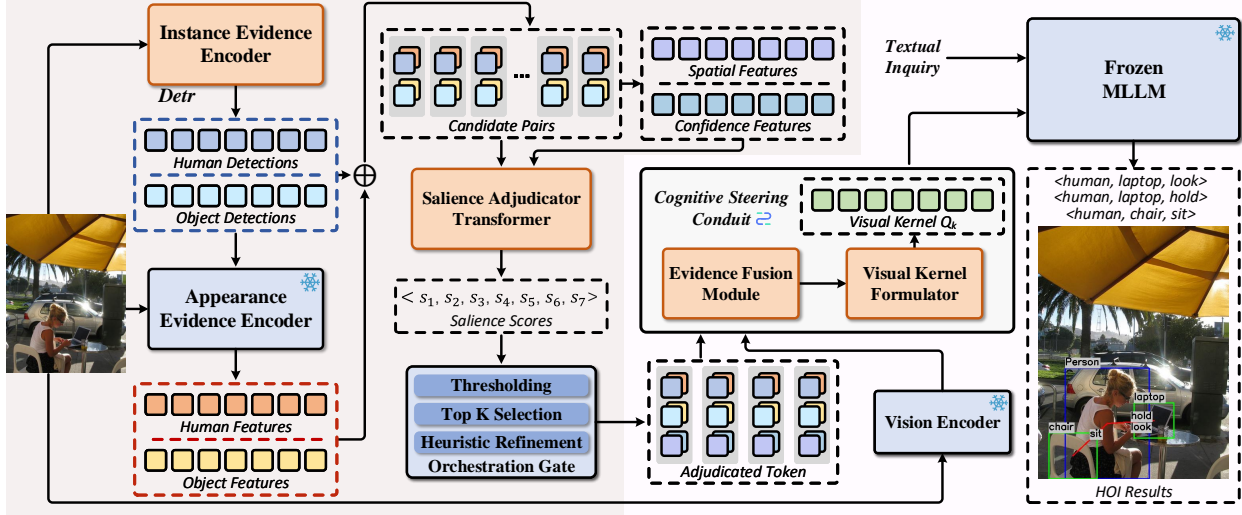


Figure 2. The architecture of GRASP-HOI, which performs open-vocabulary HOI detection by first process multi-source representations then steering a frozen generative model to describe them. The Instance Evidence Encoder and Appearance Evidence Encoder provide identified humans and objects in the image and extract visual features from the detected human, object, and their bounding box. Then a salience adjudication transformer and an Orchestration Gate distill the set of interaction features. The Cognitive Steering Conduit adjudicated candidate token with a global scene token from the frozen MLLM vision encoder into an evidence vector  $e_k$ . The visual kernel formulator transduces  $e_k$  into a sequential visual kernel  $Q_k$  to finally guide the frozen MLLM. This process enables GRASP-HOI to leverage a powerful, frozen MLLM for HOI detection with minimal, targeted training.

The function  $\mathcal{G}$  computes a low-dimensional vector representing the geometric relationship between entities, including their normalized distance, scale, and overlap. The precise definition is deferred to the appendix.

**Synergistic Adjudication.** Let  $\mathcal{P} = \{(h_k, o_k)\}_{k=1}^N$  be the set of all human-object pairs. For each candidate  $k$ , we aggregate its evidence into a single token  $u_k$  by concatenating their entity representations  $(f_h, f_o)$  and geometry  $g_k$ , followed by linear projection to the SAT dimension  $d_{\text{model}}$ . The resulting sequence  $\{u_k\}_{k=1}^N$  is fed into the salience adjudication transformer (SAT), a stack of transformer encoder layers with multi-head self-attention and feed-forward blocks. SAT performs scene-level contextual reasoning that each candidate attends to all others to capture patterns such as competition for the same object or mutually exclusive poses, and produces contextualized tokens  $\tilde{u}_k$ .

The shared linear head followed by a sigmoid maps each  $\tilde{u}_k$  to a raw salience score

$$s_k = \sigma(w_s^\top \tilde{u}_k + b_s), \quad (3)$$

reflecting the model belief that candidate  $k$  corresponds to a valid interaction. To incorporate low-level evidence quality, the Orchestration Gate (OG) combines  $s_k$  with detector confidences  $\text{conf}_h^k$  and  $\text{conf}_o^k$  into a refined score

$$r_k = \alpha s_k + (1 - \alpha) \min(\text{conf}_h^k, \text{conf}_o^k), \quad (4)$$

where  $\alpha$  is a balancing hyperparameter. We then apply

simple per-human quotas and coverage heuristics to select a compact candidate set  $\mathcal{P}^*$ . For each  $(h_k, o_k) \in \mathcal{P}^*$ , we denote its contextualized token as  $v_k$  and refer to it as the adjudicated candidate token, which serves as structured visual evidence for the subsequent cognitive steering stage.

### 3.3. Cognitive Steering Conduit

The cognitive steering stage translates the adjudicated perceptual evidence into fine-grained instructions for the frozen MLLM. While The SAT token  $\tilde{u}_k$  captures local interaction evidence and candidate-wise context, the vision tower from MLLM provides a global scene token capturing high-level semantics aligned with the text space. The Evidence Fusion Module aligns and compresses them into a compact evidence vector, then the visual kernel formulator unfolds this vector into a sequence of visual kernel tokens for precise control over the generative process.

**Evidence Fusion.** For each selected candidate  $(h_k, o_k) \in \mathcal{P}^*$ , we take its adjudicated token  $v_k$  as the local interaction evidence. To complement this with global semantics aligned to the MLLM, we extract a global scene token  $f_{\text{global}} \in \mathbb{R}^{D_g}$  from the frozen MLLM vision encoder by average pooling its last-layer patch features. Since  $v_k$  and  $f_{\text{global}}$  lie in heterogeneous feature spaces, we first project them to the MLLM hidden dimension  $d$  and then fuse them with a shallow

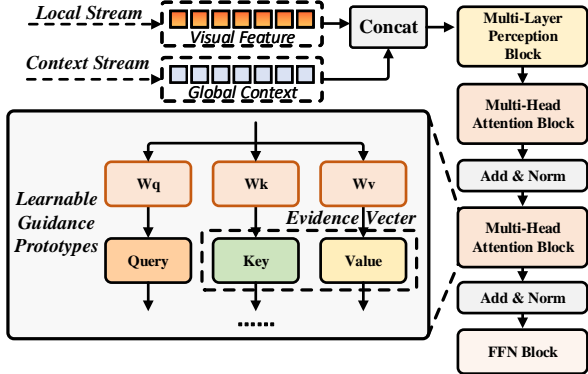


Figure 3. The architecture of Cognitive Steering Conduit. The evidence fusion module produces unified evidence vector  $e_k$ . The visual kernel formulator then transduces  $e_k$  into the visual kernel  $Q_k \in \mathbb{R}^{L \times d}$  which serves as a soft visual prefix to steer the frozen MLLM.

MLP:

$$e_k = \text{MLP}_{\text{fuse}} \left( [\phi_c(v_k) \parallel \phi_g(f_{\text{global}})] \right) \in \mathbb{R}^d, \quad (5)$$

where  $\phi_c(\cdot)$  and  $\phi_g(\cdot)$  are small projection MLPs and  $[\cdot \parallel \cdot]$  denotes concatenation. The resulting  $e_k$  is a compact, candidate-specific evidence vector expressed directly in the MLLM latent space, which serves as the sole input to the subsequent visual kernel formulator.

**Visual Kernel Formulation.** The visual kernel formulator (VKF) a lightweight cross-attention module, transduces the dense evidence vector  $e_k$  into a structured, sequential condition for the MLLM.

$$Q_k = \text{FFN}(\text{MHCA}(Z, e_k)) \in \mathbb{R}^{L \times d}. \quad (6)$$

MHCA uses  $e_k$  as a shared memory (key/value) for all slots;  $L$  controls prompt capacity. The resulting  $Q_k$  is the candidate’s visual kernel that conditions the MLLM to reason about the specific interaction.

**Kernel-Conditioned Generation.** The generated visual kernel  $Q_k$  is prepended to the token embeddings of a textual inquiry to form a unified input sequence for the frozen MLLM. Let  $E(\cdot)$  be the text embedding layer and  $T$  tokens of inquiry text, the final input sequence is given by:

$$\tilde{X}_k = [Q_k, E(\text{text})] \in \mathbb{R}^{(L+T) \times d}. \quad (7)$$

Within the autoregressive process of MLLM, the attention mechanism ensures that every subsequently generated text token attends to the prefixed visual kernel.  $Q_k$  thus acts as persistent visual condition, steering the generation process to elaborate on the specific visual hypothesis it represents, rather than answering generic question.

### 3.4. Training Objective

We jointly optimize all learnable components under a unified multi-task objective, while keeping the MLLM and DINO encoders frozen. The overall loss is defined as

$$\begin{aligned} \mathcal{L} = & \lambda_{\text{det}} \mathcal{L}_{\text{det}} + \lambda_{\text{sal}} \mathcal{L}_{\text{sal}} \\ & + \lambda_{\text{gen}} \mathcal{L}_{\text{gen}} + \lambda_{\text{nce}} \mathcal{L}_{\text{nce}} + \lambda_{\text{logic}} \mathcal{L}_{\text{logic}}, \end{aligned} \quad (8)$$

where  $\lambda$  are weighting coefficients.  $\mathcal{L}_{\text{det}}$  follows the standard set-based detection loss used in query-based detectors, and  $\mathcal{L}_{\text{sal}}$  is a binary cross-entropy loss with Hungarian matching that trains the SAT to predict salient candidates.

**Generative Consistency  $\mathcal{L}_{\text{gen}}$ .** For a positive candidate, given its ground-truth verb phrase  $y_{1:T}$ , we enforce

$$\mathcal{L}_{\text{gen}} = - \sum_{t=1}^T \log p(y_t \mid y_{<t}, Q_k), \quad (9)$$

with decoding restricted to a verb-focused vocabulary during training, ensuring that  $Q_k$  genuinely controls the generated verb sequence.

**Semantic Alignment  $\mathcal{L}_{\text{nce}}$ .** We align kernels and verbs inside the same MLLM text–visual embedding space. Let  $\bar{Q}_k = \frac{1}{L} \sum_{\ell=1}^L Q_k^{(\ell)}$ ,  $w^+$  be the frozen text embedding of the ground-truth verb and  $\mathcal{W}^-$  negatives. We use InfoNCE:

$$\mathcal{L}_{\text{nce}} = - \log \frac{\exp(\cos(\bar{Q}_k, w^+)/\tau)}{\sum_{w \in \{w^+\} \cup \mathcal{W}^-} \exp(\cos(\bar{Q}_k, w)/\tau)}. \quad (10)$$

This is analogous to CLIP-style alignment, but with the visual kernel serving as the visual side.

**Logical Consistency  $\mathcal{L}_{\text{logic}}$ .** We inject commonsense via a soft mutual-exclusion regularizer. For mutually exclusive verb pairs  $\mathcal{M}$  (e.g., *sit on* vs. *stand on*), let  $p(v \mid Q_k)$  be the probability of generating the canonical prompt of  $v$  under teacher forcing (using the first verb token’s softmax). Then

$$\mathcal{L}_{\text{logic}} = \sum_{(v, v') \in \mathcal{M}} \min(p(v \mid Q_k), p(v' \mid Q_k)). \quad (11)$$

This penalizes assigning high probabilities to logically incompatible verbs without modifying MLLM parameters.

### 3.5. Real-time Inference with GRASP-HOI

**Constrained Decoding.** For each  $(h_k, o_k) \in \mathcal{P}^*$ , the MLLM generates a short description under  $Q_k$ . To ensure reproducible evaluation, we use constrained decoding over the verb set  $\mathcal{V}$  (and minimal auxiliaries) and apply a simple template-based rule to extract the main verb, yielding  $\langle b_{h_k}, v_k, b_{o_k} \rangle$ . We find constrained decoding crucial to mitigate semantic drift and stabilize metrics.

**Open-Vocabulary Mapping.** For open-vocabulary evaluation, we relax the constraint, mapping the generated phrase to canonical verb via cosine similarity in the frozen MLLM text embedding space (the same space used by  $\mathcal{L}_{\text{nce}}$ ), optionally filtered by WordNet synonyms.

## 4. Experiments

### 4.1. Datasets and Evaluation Metrics

**HICO-DET.** HICO-DET [6] is a large-scale HOI detection benchmark containing 47776 images with 80 object categories, 117 verbs, and 600 interaction triplets. We follow the standard split, using 38118 images for training and 9658 for testing. Following prior works, we report mean average precision (mAP) under two evaluation settings: *Default*, where undetected objects are treated as negatives, and *Known Object*, where ground-truth object boxes are given. For both settings, we further break down mAP into Full, Rare, and Non-rare categories, where Rare triplets have fewer than 10 training instances.

**V-COCO.** V-COCO [10] is built upon MS-COCO and contains 10346 images annotated with 26 action classes. We adopt the official dataset splits and follow the standard evaluation protocol using  $\text{AP}_1^{\text{role}}$  and  $\text{AP}_2^{\text{role}}$ . A prediction is counted as correct only if both the human and object boxes and the action label are correct;  $\text{AP}_2^{\text{role}}$  further considers cases with multiple objects per action.

**Zero-shot and Open-vocabulary Evaluation.** To evaluate open-vocabulary performance on HICO-DET, we follow the widely adopted zero-shot protocols including (i) *Unseen Composition* (UC), where a subset of  $\langle \text{human}, \text{verb}, \text{object} \rangle$  triplets are held out while their verbs and objects remain seen; (ii) *Unseen Object* (UO), where some object categories never appear during training; and (iii) *Unseen Verb* (UV), where certain verbs are unseen. For each setting, we report mAP on the unseen, seen, and full splits.

### 4.2. Implementation Details

GRASP-HOI is built on query-based detector (DETR) for human/object proposals and a frozen vision backbone (DINOv3) for appearance tokens. We used InternVL3.5 as the frozen MLLM backbone of our framework. We set  $L$ ,  $K$ ,  $\alpha$ , and  $(\lambda_{\text{gen}}, \lambda_{\text{nce}}, \lambda_{\text{logic}})$  to 8, 3, 0.6, and  $(1.0, 0.5, 0.1)$ , respectively. We train GRASP-HOI using AdamW with a weight decay of  $10^{-4}$  and a cosine learning rate schedule. All experiments are conducted with a batch size of 16 on 8 NVIDIA A6000 GPUs.

### 4.3. Comparison with State-of-the-Arts

**Closed-Set Performance.** We first compare GRASP-HOI with state-of-the-art (SOTA) methods on the standard HICO-DET and V-COCO datasets, with results summarized in Table 1. On the challenging HICO-DET default setting, our method establishes a new SOTA, achieving 48.02 mAP in full split, surpassing the previous leading method, HORN (47.53 mAP) by +0.49 mAP. Notably, the capability of our generative framework is revealed in the long-tail rare split. GRASP-HOI achieves 48.15 mAP, establishing +1.34 mAP lead over HORN. While many recent methods achieve gains primarily by optimizing for the non-rare set, the improvement on the data-sparse rare set provides compelling evidence for our approach. It validates that our cognitive steering paradigm by effectively leveraging the rich, implicit world knowledge of the frozen MLLM, successfully breaks away from the spurious correlations that plague traditional classifiers in the long-tail distribution. This robust performance is also shown on V-COCO dataset, where GRASP-HOI also achieves state-of-the-art performance in  $\text{AP}_{\text{role}}^{\#1}$  and  $\text{AP}_{\text{role}}^{\#2}$  respectively, confirming the broad applicability and robustness of our framework.

**Open-Vocabulary Performance.** We evaluate the central hypothesis of our work with the model capacity to generalize to unseen interactions, which is a fundamental limitation of closed-world detectors. Table 2 presents the comprehensive evaluation across the four standard zero-shot settings on HICO-DET. The most challenging setting is the unseen verb (UV) split, as it directly tests the ability to reason about and generate novel action semantics not present in the training data. In this challenging split, GRASP-HOI achieves 32.45 mAP on unseen verbs, outperforming the strong baseline BC-HOI (31.18 mAP) by +1.27 mAP. This result quantitatively demonstrates that our generative reformulation effectively breaks the closed-world assumption, producing valid inferences for verbs unseen during training. Also the superior generalization extends across all settings. In rare first unseen combination, our model achieves 43.67 mAP, surpassing BC-HOI by +1.36 mAP. We observe similar SOTA results in the NF-UC (35.61 mAP) and UO (39.98 mAP) settings. The consistent dominance across all four settings underscores the fundamental advantage of our generative reasoning paradigm, moving beyond simple matching to achieve true open-vocabulary understanding.

### 4.4. Ablation Studies

We perform series of ablation studies on HICO-DET with default full setting to dissect the GRASP-HOI framework and quantify each module contribution. Our

Table 1. Comparison with state-of-the-art methods on HICO-DET and V-COCO in the closed-set setting. We report mAP (%) and sort methods by HICO-DET Default Full.

Method	Backbone	HICO-DET Default			HICO-DET Known-Object			V-COCO	
		Full	Rare	Non-Rare	Full	Rare	Non-Rare	$AP_{role}^{\#1}$	$AP_{role}^{\#2}$
QPIC [35]	ResNet-101	29.90	23.92	31.69	32.38	26.06	34.27	58.8	61.0
CDN [54]	ResNet-50	31.78	27.55	33.05	34.53	29.73	35.96	62.3	64.4
UPT [18]	ResNet-101	32.62	28.62	33.81	36.08	31.41	37.47	61.3	67.1
RLIP [51]	ResNet-50	32.84	26.85	34.63	—	—	—	61.9	64.2
GEN-VLKT [23]	R50+CLIP	33.75	29.25	35.10	36.78	32.75	37.99	62.4	64.7
HOICLIP [32]	ResNet-50	34.69	31.12	35.74	37.61	34.47	38.54	63.5	64.8
CLIP4HOI [30]	ResNet-50	35.33	33.95	35.74	37.19	35.27	37.77	—	66.3
CQL [44]	ResNet-101	36.03	33.16	36.89	38.82	35.51	39.81	66.5	69.9
DP-HOI [22]	ResNet-50	36.56	34.36	37.22	39.37	36.59	40.20	66.6	—
AGER [37]	ResNet-50	36.75	33.53	37.71	39.84	35.58	40.23	65.7	69.7
FGAHOI [28]	Swin-L	37.18	30.71	39.11	38.93	31.93	41.02	60.5	61.2
VIPLO [33]	R50+CLIP	37.22	35.45	37.75	40.61	38.82	41.15	62.2	68.0
RmLR [5]	ResNet-101	37.41	28.81	39.97	38.69	31.27	40.91	64.2	70.2
CMMMP [20]	ResNet-50	38.14	37.75	38.25	—	—	—	—	64.0
ADA-CM [18]	R50+CLIP	38.40	37.52	38.66	—	—	—	58.6	64.0
EZ-HOI [16]	ResNet-50	38.61	37.70	38.89	—	—	—	60.5	66.2
BCOM [40]	ResNet-50	39.34	39.90	39.17	42.24	42.86	42.05	65.8	69.9
UniHOI-1 [4]	R101+ViT-L	40.95	40.27	41.32	43.26	43.12	43.25	68.1	70.8
DiffHOI [49]	Swin-L	41.50	39.96	41.96	43.62	41.41	44.28	65.7	68.2
BC-HOI [12]	ResNet-50	43.01	45.76	42.18	45.35	47.94	44.57	68.2	70.1
PVIC [57]	Swin-L	44.32	44.61	44.24	47.81	48.38	47.64	64.1	70.2
MP-HOI [50]	Swin-L+ViT	44.53	44.48	44.55	—	—	—	66.2	67.6
SICHOI [26]	R101+ViT-L	45.04	45.61	44.88	48.16	48.37	48.09	71.1	75.6
RLIPv2 [52]	Swin-L	45.09	43.23	45.64	—	—	—	72.1	74.1
PAFR [41]	Swin-L	46.01	46.74	45.80	49.50	50.59	49.18	63.0	68.7
HORP [7]	Swin-L+CLIP	47.53	46.81	47.74	51.24	50.78	51.38	68.9	71.1
<b>GRASP-HOI (Ours)</b>	<b>ResNet-50+MLM</b>	<b>48.02</b>	<b>48.15</b>	<b>48.09</b>	<b>51.57</b>	<b>51.53</b>	<b>51.61</b>	<b>72.5</b>	<b>76.2</b>

Table 2. Open-vocabulary evaluation on HICO-DET. Performance is measured in mAP under four zero-shot settings: Rare First Unseen Combination (RF-UC), Non-rare First Unseen Combination (NF-UC), Unseen Object (UO), and Unseen Verb (UV).

Method	RF-UC			NF-UC			UO			UV		
	Unseen	Seen	Full									
GEN-VLKT [23]	21.36	32.91	30.56	25.05	23.38	23.71	10.51	28.92	25.63	20.96	30.23	28.74
RLIPv2-ParSeDA[23]	21.45	35.85	32.97	22.81	29.52	28.18	—	—	—	—	—	—
HOICLIP [32]	25.53	34.85	32.99	26.39	28.10	27.75	16.20	30.99	28.53	24.30	32.19	31.09
DP-HOI [22]	30.49	36.17	35.03	28.87	29.98	29.76	—	—	—	26.30	34.49	33.34
DiffHOI [49]	32.06	36.77	35.89	—	—	—	—	—	—	—	—	—
BCOM [40]	—	—	—	33.12	31.76	32.03	—	—	—	—	—	—
HOIGen [9]	—	—	—	33.98	32.86	33.08	36.35	32.90	33.48	20.27	34.31	32.34
UniHOI (BLIP2) [4]	28.68	33.16	32.27	28.45	32.63	31.79	19.72	34.76	31.56	26.05	36.78	34.68
EZ-HOI [16]	34.24	37.35	36.73	—	—	—	38.17	36.02	36.38	28.82	38.15	36.84
CMMMP [20]	35.98	37.42	37.13	33.52	35.53	35.13	39.67	36.15	36.74	30.84	37.28	36.38
SICHOI [26]	34.24	41.58	40.11	34.52	36.06	35.75	—	—	—	—	—	—
BC-HOI [12]	42.31	40.67	40.99	33.01	37.24	36.40	19.94	37.03	34.18	31.18	41.31	39.89
<b>GRASP-HOI (Ours)</b>	<b>43.67</b>	<b>42.98</b>	<b>42.46</b>	<b>35.61</b>	<b>38.95</b>	<b>38.24</b>	<b>39.98</b>	<b>38.15</b>	<b>37.69</b>	<b>32.45</b>	<b>42.57</b>	<b>40.14</b>

Table 3. Ablation studies of core components of GRASP-HOI on HICO-DET (Default Full).  $\mathcal{L}_{\text{nce}}$ ,  $\mathcal{L}_{\text{gen}}$  and CSC denote the alignment loss, generative loss, and cognitive steering conduit.

Method	$\mathcal{L}_{\text{nce}}$	$\mathcal{L}_{\text{gen}}$	CSC	mAP
Baseline (Classifier)	-	-	-	31.8
+ Alignment Loss	✓	-	-	43.7
+ Generative Loss	✓	✓	-	46.5
+ CSC (Full Model w/o $\mathcal{L}_{\text{logic}}$ )	✓	✓	✓	47.7
<b>GRASP-HOI (Full)</b>	✓	✓	✓	<b>48.02</b>

Table 4. Ablation studies of the key components in cognitive steering conduit on HICO-DET (Default Full).

CSC Configuration	mAP
<b>Full Model (Local + Global + VKF)</b>	<b>48.02</b>
w/o Global Evidence ( $f_{\text{global}}$ )	46.1
w/o Local Evidence ( $v_k$ )	41.3
w/ Naive Fusion (replace VKF with MLP)	44.6

analysis is structured to validate three central hypotheses: first, the superiority of our generative paradigm over traditional classification; second, the critical role of the cognitive steering conduit (CSC) as the core steering mechanism; and third, the synergistic effect of our hybrid guidance losses.

**Analysis of Core Components.** We validate our design via incremental build-up study in Table 3. We start with a non-generative baseline classifier, using the SAT output with a standard classification head, which yields 31.8 mAP. Replacing the classifier with our generative framework and using only the semantic alignment loss ( $\mathcal{L}_{\text{nce}}$ ) boosts performance to 43.7 mAP (+11.9), confirming the benefit of leveraging the MLLM latent space. Next, introducing the generative consistency loss ( $\mathcal{L}_{\text{gen}}$ ) to force autoregressive verb prediction adds another +2.8 mAP, demonstrating that fine-grained generative supervision is critical for accuracy. Incorporating our full cognitive steering conduit (CSC) provides the largest gain of +1.52 mAP, identifying the CSC as the principal driver of performance. This confirms our designation that visual evidence is structured for the MLLM as is critical as the evidence itself. Finally, adding the  $\mathcal{L}_{\text{logic}}$  loss provides final +0.32 mAP refinement, bringing the model to its peak performance of 48.02 mAP by regularizing against commonsense-violating predictions.

**Dissection of the Cognitive Steering Conduit.** Having established the CSC as the principal performance driver, we now dissect its internal architecture in Table 4 to isolate the contribution of each component. Removing the global scene token  $f_{\text{global}}$  yields a notable 1.9

Table 5. Effect of the visual kernel length  $L$  in the CSC on HICO-DET (Default Full). Vary  $L$  from 1 to 16 and report mAP (%).

Kernel Length ( $L$ )	1	4	8	16
<b>HICO-DET (mAP)</b>	45.9	47.3	<b>48.02</b>	48.01

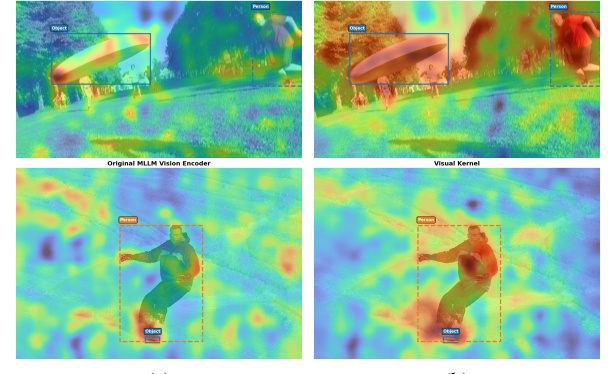


Figure 4. Qualitative visualization of the steering effect of the Cognitive Steering Conduit (CSC) on HICO-DET. (a) Attention from the frozen vision encoder is diffuse and often focuses on irrelevant regions. (b) Our visual kernel yields concentrated responses on the target human-object interaction regions.

mAP reduction, confirming that holistic scene cues remain indispensable for resolving ambiguous or multi-object interactions. Eliminating the local adjudicated token  $v_k$  leads to a dramatic collapse to 41.3 mAP, underscoring that specific multi-source features is the core steering signal that enables precise reasoning within the MLLM. Finally, substituting our visual kernel formulator (VKF) with a naive MLP projection further degrades performance to 44.6 mAP. This degradation highlights a key insight that simple feature projection cannot faithfully expose the perceptual structure required for generation, whereas the cross-attention design is critical for grounding and shaping an effective generative condition.

**Hyperparameter Analysis of Visual Kernel Length.** We further examine the sensitivity to the kernel length  $L$ , a key hyperparameter of the CSC, as shown in Table 5. Performance peaks at  $L=8$ . Shorter kernels ( $L \leq 4$ ) provide insufficient capacity to encode fine-grained visual cues, resulting in noticeable degradation. In contrast, extending the kernel to  $L=16$  yields marginal gains while introducing additional computation. These results indicate that  $L=8$  offers the most favorable balance between representational expressiveness and parameter efficiency, serving as the optimal configuration for stable generation.

#### 4.5. Qualitative Analysis

We present qualitative visualizations of attention maps in Figure 4 to compare the responses of the frozen

vision encoder in MLLM with produced after injecting candidate-specific visual kernel. The frozen encoder generally distributes attention broadly across background regions or non-interacting entities, reflecting its generic pre-training objectives. After applying visual kernel, the attention becomes sharply concentrated around the target human-object pair, highlighting both the interaction region and the supporting visual cues required for correct reasoning. This focused pattern demonstrates the visual kernel functions as an effective steering signal, grounding the MLLM’s high-level representations in the relevant perceptual evidence and reasoning capability. These visualizations provide intuitive confirmation that CSC enables the model to align generative reasoning with fine-grained, interaction-centric visual context.

## 5. Conclusion

In this paper, we present GRASP-HOI, a framework that reformulates human-object interaction (HOI) detection from closed-set classification to open-vocabulary generative reasoning. At the core of our approach is the cognitive steering conduit (CSC), a lightweight and differentiable module that injects structured, candidate-specific visual evidence to steer a frozen multimodal large language model (MLLM). Enabled by a hybrid guidance strategy, the CSC leverages the MLLM’s reasoning capability without requiring any model fine-tuning. Extensive experiments show that GRASP-HOI achieves new state-of-the-art performance in both standard closed-set and open-vocabulary settings, demonstrating a superior and efficient paradigm that effectively bridges the long-standing gap between discriminative perception and high-level cognitive reasoning.

## References

- [1] Josh Achiam, Steven Adler, Sandhini Agarwal, Lama Ahmad, Ilge Akkaya, Florencia Leoni Aleman, Diogo Almeida, Janko Altenschmidt, Sam Altman, Shyamal Anadkat, et al. Gpt-4 technical report. *arXiv preprint arXiv:2303.08774*, 2023. 1
- [2] Jinze Bai, Shuai Bai, Shusheng Yang, Shijie Wang, Sinan Tan, Peng Wang, Junyang Lin, Chang Zhou, and Jingen Zhou. Qwen-vl: A versatile vision-language model for understanding, localization, text reading, and beyond. *arXiv preprint arXiv:2308.12966*, 2023. 3
- [3] Shuai Bai, Keqin Chen, Xuejing Liu, Jialin Wang, Wenbin Ge, Sibo Song, Kai Dang, Peng Wang, Shijie Wang, Jun Tang, et al. Qwen2.5-vl technical report. *arXiv preprint arXiv:2502.13923*, 2025. 1
- [4] Yichao Cao, Qingfei Tang, and Xiu Su. Detecting any human-object interaction relationship: universal hoi detector with spatial prompt learning on foundation models. In *Proceedings of the Advances in Neural Information Processing Systems (NeurIPS)*, 2023. 2, 7
- [5] Yichao Cao, Qingfei Tang, Feng Yang, Xiu Su, Shan You, Xiaobo Lu, and Chang Xu. Re-mine, learn and reason: exploring the cross-modal semantic correlations for language-guided hoi detection. In *Proceedings of the IEEE/CVF International Conference on Computer Vision (ICCV)*, pages 23435–23446, 2023. 1, 7
- [6] Yu-Wei Chao, Yunfan Liu, Xieyang Liu, Huayi Zeng, and Jia Deng. Learning to detect human-object interactions, 2018. 6
- [7] Pei Geng, Jian Yang, and Shanshan Zhang. Horp: human-object relation priors guided hoi detection. In *Proceedings of the IEEE/CVF Conference on Computer Vision and Pattern Recognition (CVPR)*, 2025. 7
- [8] Georgia Gkioxari, Ross Girshick, Piotr Dollár, and Kaiming He. Detecting and recognizing human-object interactions. In *Proceedings of the IEEE conference on computer vision and pattern recognition*, pages 8359–8367, 2018. 1
- [9] Yixin Guo, Yu Liu, Jianghao Li, Weimin Wang, and Qi Jia. Unseen no more: Unlocking the potential of clip for generative zero-shot hoi detection. In *Proceedings of the ACM International Conference on Multimedia*, pages 1711–1720, 2024. 7
- [10] Saurabh Gupta and Jitendra Malik. Visual semantic role labeling. *arXiv preprint arXiv:1505.04474*, 2015. 6
- [11] Geng Han, Jiachen Zhao, Lele Zhang, and Fang Deng. A survey of human-object interaction detection with deep learning. *IEEE Transactions on Emerging Topics in Computational Intelligence*, 9(1):3–26, 2025. 1, 2
- [12] Yupeng Hu, Changxing Ding, Chang Sun, Shaoli Huang, and Xiangmin Xu. Bilateral collaboration with large vision-language models for open vocabulary human-object interaction detection. In *Proceedings of the IEEE/CVF International Conference on Computer Vision*, pages 20126–20136, 2025. 2, 3, 7
- [13] Bumsoo Kim, Junhyun Lee, Jaewoo Kang, Eun-Sol Kim, and Hyunwoo J. Kim. Hotr: End-to-end human-object interaction detection with transformers. In *Proceedings of the IEEE/CVF Conference on Computer Vision and Pattern Recognition (CVPR)*, pages 74–83, 2021. 2
- [14] Ho-Joong Kim, Jung-Ho Hong, Heejo Kong, and Seong-Whan Lee. Te-tad: towards full end-to-end temporal action detection via time-aligned coordinate expression. In *Proceedings of the IEEE/CVF Conference on Computer Vision and Pattern Recognition (CVPR)*, pages 18837–18846, 2024. 1
- [15] Sanghyun Kim, Deunsol Jung, and Minsu Cho. Locality-aware zero-shot human-object interaction detection. In *Proceedings of the IEEE/CVF Conference on Computer Vision and Pattern Recognition (CVPR)*, pages 20190–20200, 2025. 3
- [16] Qinqian Lei, Bo Wang, and Robby Tan. Ez-hoi: Vlm adaptation via guided prompt learning for zero-shot hoi detection. *Proceedings of the Advances in Neural Information Processing Systems (NeurIPS)*, 37:55831–55857, 2024. 7
- [17] Qinqian Lei, Bo Wang, and Robby T Tan. Hola: Zero-shot hoi detection with low-rank decomposed vlm fea-

ture adaptation. In *Proceedings of the IEEE/CVF International Conference on Computer Vision (ICCV)*, pages 1825–1835, 2025. 3

[18] Ting Lei, Fabian Caba, Qingchao Chen, Hailin Jin, Yuxin Peng, and Yang Liu. Efficient adaptive human-object interaction detection with concept-guided memory. In *Proceedings of the IEEE/CVF International Conference on Computer Vision (ICCV)*, pages 6457–6467, 2023. 7

[19] Ting Lei, Shaofeng Yin, and Yang Liu. Exploring the potential of large foundation models for open-vocabulary hoi detection. In *Proceedings of the IEEE/CVF Conference on Computer Vision and Pattern Recognition (CVPR)*, 2024. 2

[20] Ting Lei, Shaofeng Yin, Yuxin Peng, and Yang Liu. Exploring conditional multi-modal prompts for zero-shot hoi detection. In *Proceedings of the European Conference on Computer Vision (ECCV)*, pages 1–19. Springer, 2024. 7

[21] Rongjie Li, Songyang Zhang, Dahua Lin, Kai Chen, and Xuming He. From pixels to graphs: Open-vocabulary scene graph generation with vision-language models. In *Proceedings of the IEEE/CVF Conference on Computer Vision and Pattern Recognition (CVPR)*, pages 28076–28086, 2024. 1

[22] Zhuolong Li, Xingao Li, Changxing Ding, and Xiangmin Xu. Disentangled pre-training for human-object interaction detection. In *Proceedings of the IEEE/CVF Conference on Computer Vision and Pattern Recognition (CVPR)*, pages 28191–28201, 2024. 3, 7

[23] Yue Liao, Aixi Zhang, Miao Lu, Yongliang Wang, Xiaobo Li, and Si Liu. Gen-vlkt: simplify association and enhance interaction understanding for hoi detection. In *Proceedings of the IEEE/CVF Conference on Computer Vision and Pattern Recognition (CVPR)*, pages 20091–20100, 2022. 7

[24] Haotian Liu, Chunyuan Li, Qingyang Wu, and Yong Jae Lee. Visual instruction tuning. *Proceedings of the Advances in Neural Information Processing Systems (NeurIPS)*, 36:34892–34916, 2023. 1

[25] Ye Liu, Junsong Yuan, and Chang Wen Chen. Consnet: learning consistency graph for zero-shot human-object interaction detection. In *Proceedings of the ACM International Conference on Multimedia*, pages 4235–4243, 2020. 2

[26] Jinguo Luo, Weihong Ren, Weibo Jiang, Xi’ai Chen, Qiang Wang, Zhi Han, and Honghai Liu. Discovering syntactic interaction clues for human-object interaction detection. In *Proceedings of the IEEE/CVF Conference on Computer Vision and Pattern Recognition (CVPR)*, pages 28212–28222, 2024. 2, 3, 7

[27] Yun Luo, Zhen Yang, Fandong Meng, Yafu Li, Jie Zhou, and Yue Zhang. An empirical study of catastrophic forgetting in large language models during continual fine-tuning. *IEEE Transactions on Audio, Speech and Language Processing*, 2025. 2

[28] Shuailei Ma, Yuefeng Wang, Shanze Wang, and Ying Wei. Fgahoi: fine-grained anchors for human-object interaction detection. *IEEE Transactions on Pattern Analysis and Machine Intelligence*, 46(4):2415–2429, 2024. 2, 7

[29] Yueen Ma, Zixing Song, Yuzheng Zhuang, Jianye Hao, and Irwin King. A survey on vision-language-action models for embodied ai. *arXiv preprint arXiv:2405.14093*, 2024. 1

[30] Yunyao Mao, Jiajun Deng, Wengang Zhou, Li Li, Yao Fang, and Houqiang Li. CLIP4HOI: Towards adapting CLIP for practical zero-shot HOI detection. In *Proceedings of the Advances in Neural Information Processing Systems (NeurIPS)*, 2023. 7

[31] Esteve Valls Mascaro, Daniel Sliwowski, and Dongheui Lee. Hoi4abot: Human-object interaction anticipation for human intention reading collaborative robots. In *Proceedings of The Conference on Robot Learning*, pages 1111–1130. PMLR, 2023. 1

[32] Shan Ning, Longtian Qiu, Yongfei Liu, and Xuming He. Hoiclip: Efficient knowledge transfer for hoi detection with vision-language models. In *Proceedings of the IEEE/CVF Conference on Computer Vision and Pattern Recognition (CVPR)*, pages 23507–23517, 2023. 2, 3, 7

[33] Jeeseung Park, Jin-Woo Park, and Jong-Seok Lee. Viplo: Vision transformer based pose-conditioned self-loop graph for human-object interaction detection. In *Proceedings of the IEEE/CVF Conference on Computer Vision and Pattern Recognition (CVPR)*, pages 17152–17162, 2023. 2, 7

[34] Weihong Ren, Jinguo Luo, Weibo Jiang, Liangqiong Qu, Zhi Han, Jiandong Tian, and Honghai Liu. Learning self- and cross-triplet context clues for human-object interaction detection. *IEEE Transactions on Circuits and Systems for Video Technology*, 34(10):9760–9773, 2024. 2

[35] Masato Tamura, Hiroki Ohashi, and Tomoaki Yoshinaga. Qpic: query-based pairwise human-object interaction detection with image-wide contextual information. In *Proceedings of the IEEE/CVF Conference on Computer Vision and Pattern Recognition (CVPR)*, pages 10405–10414, 2021. 7

[36] Hugo Touvron, Thibaut Lavril, Gautier Izacard, Xavier Martinet, Marie-Anne Lachaux, Timothée Lacroix, Baptiste Rozière, Naman Goyal, Eric Hambro, Faisal Azhar, et al. Llama: Open and efficient foundation language models. *arXiv preprint arXiv:2302.13971*, 2023. 1

[37] Danyang Tu, Wei Sun, Guangtao Zhai, and Wei Shen. Agglomerative transformer for human-object interaction detection. In *Proceedings of the IEEE/CVF International Conference on Computer Vision (ICCV)*, pages 21614–21624, 2023. 7

[38] Ashish Vaswani, Noam Shazeer, Niki Parmar, Jakob Uszkoreit, Llion Jones, Aidan N. Gomez, Łukasz Kaiser, and Illia Polosukhin. Attention is all you need. *arXiv preprint arXiv:1706.03762*, 2017. 3

[39] Bo Wan and Tinne Tuytelaars. Exploiting clip for zero-shot hoi detection requires knowledge distillation at multiple levels. In *Proceedings of the IEEE/CVF Winter Conference on Applications of Computer Vision*, pages 1805–1815, 2024. 3

[40] Guangzhi Wang, Yangyang Guo, Ziwei Xu, and Mohan Kankanhalli. Bilateral adaptation for human-object interaction detection with occlusion-robustness. In *Proceedings of the IEEE/CVF Conference on Computer Vision and Pattern Recognition (CVPR)*, pages 27970–27980, 2024. 2, 7

[41] Eastman Z Y Wu, Yali Li, Yuan Wang, and Shengjin Wang. Exploring pose-aware human-object interaction via hybrid learning. In *Proceedings of the IEEE/CVF Conference on Computer Vision and Pattern Recognition (CVPR)*, pages 17815–17825, 2024. 7

[42] Mingrui Wu, Jiaxin Gu, Yunhang Shen, Mingbao Lin, Chao Chen, and Xiaoshuai Sun. End-to-end zero-shot hoi detection via vision and language knowledge distillation. In *Proceedings of the AAAI conference on artificial intelligence*, pages 2839–2846, 2023. 3

[43] Mingrui Wu, Yuqi Liu, Jiayi Ji, Xiaoshuai Sun, and Rongrong Ji. Toward open-set human object interaction detection. In *Proceedings of the AAAI Conference on Artificial Intelligence*, pages 6066–6073, 2024. 2

[44] Chi Xie, Fangao Zeng, Yue Hu, Shuang Liang, and Yichen Wei. Category query learning for human-object interaction classification. In *Proceedings of the IEEE/CVF Conference on Computer Vision and Pattern Recognition (CVPR)*, pages 15275–15284, 2023. 7

[45] Baochen Xiong, Xiaoshan Yang, Yaguang Song, Yaowei Wang, and Chang Sheng Xu. Modality-collaborative test-time adaptation for action recognition. In *Proceedings of the IEEE/CVF Conference on Computer Vision and Pattern Recognition (CVPR)*, pages 26722–26731, 2024. 1

[46] Weiyang Xue, Qi Liu, Qiwei Xiong, Yuxiao Wang, Zhenao Wei, Xiaofen Xing, and Xiangmin Xu. Towards zero-shot human-object interaction detection via vision-language integration. *neural networks*, 2025. 3

[47] An Yang, Baosong Yang, Beichen Zhang, Binyuan Hui, Bo Zheng, Bowen Yu, Chengyuan Li, Dayiheng Liu, Fei Huang, Haoran Wei, et al. Qwen2.5 technical report. *arXiv preprint arXiv:2412.15115*, 2024. 3

[48] An Yang, Anfeng Li, Baosong Yang, Beichen Zhang, Binyuan Hui, Bo Zheng, Bowen Yu, Chang Gao, Chen-gen Huang, Chenxu Lv, et al. Qwen3 technical report. *arXiv preprint arXiv:2505.09388*, 2025. 1

[49] Jie Yang, Bingliang Li, Fengyu Yang, Ailing Zeng, Lei Zhang, and Ruimao Zhang. Boosting human-object interaction detection with text-to-image diffusion model. *arXiv preprint arXiv:2305.12252*, 2023. 7

[50] Jie Yang, Bingliang Li, Ailing Zeng, Lei Zhang, and Ruimao Zhang. Open-world human-object interaction detection via multi-modal prompts. In *Proceedings of the IEEE/CVF Conference on Computer Vision and Pattern Recognition (CVPR)*, 2024. 2, 3, 7

[51] Hangjie Yuan, Jianwen Jiang, Samuel Albanie, Tao Feng, Ziyuan Huang, Dong Ni, and Mingqian Tang. Rlip: relational language-image pre-training for human-object interaction detection. In *Proceedings of the Advances in Neural Information Processing Systems (NeurIPS)*, 2022. 1, 3, 7

[52] Hangjie Yuan, Shiwei Zhang, Xiang Wang, Samuel Albanie, Yining Pan, Tao Feng, Jianwen Jiang, Dong Ni, Yingya Zhang, and Deli Zhao. Rlipv2: Fast scaling of relational language-image pre-training. In *Proceedings of the IEEE/CVF International Conference on Computer Vision (ICCV)*, pages 21592–21604, 2023. 2, 7

[53] Yu-Wei Zhan, Fan Liu, Xin Luo, Xin-Shun Xu, Liqiang Nie, and Mohan Kankanhalli. Enhancing hoi detection with contextual cues from large vision-language models. In *Proceedings of the ACM International Conference on Multimedia*, pages 8557–8566, 2025. 3

[54] Aixi Zhang, Yue Liao, Si Liu, Miao Lu, Yongliang Wang, Chen Gao, and Xiaobo Li. Mining the benefits of two-stage and one-stage hoi detection. *Proceedings of the Advances in Neural Information Processing Systems (NeurIPS)*, 34:17209–17220, 2021. 7

[55] Ce Zhang, Simon Stepputtis, Joseph Campbell, Katia Sycara, and Yaqi Xie. Hiker-sgg: hierarchical knowledge enhanced robust scene graph generation. In *Proceedings of the IEEE/CVF Conference on Computer Vision and Pattern Recognition (CVPR)*, pages 28233–28243, 2024. 1

[56] Frederic Z. Zhang, Dylan Campbell, and Stephen Gould. Efficient two-stage detection of human-object interactions with a novel unary-pairwise transformer. In *Proceedings of the IEEE/CVF Conference on Computer Vision and Pattern Recognition (CVPR)*, pages 20072–20080, 2022. 2

[57] Frederic Z Zhang, Yuhui Yuan, Dylan Campbell, Zhuoyao Zhong, and Stephen Gould. Exploring predicate visual context in detecting of human-object interactions. In *Proceedings of the IEEE/CVF International Conference on Computer Vision (ICCV)*, pages 10411–10421, 2023. 7

[58] Hang Zhang, Xin Li, and Lidong Bing. Video-llama: An instruction-tuned audio-visual language model for video understanding. *arXiv preprint arXiv:2306.02858*, 2023. 3

[59] Kaiyan Zhang, Yuxin Zuo, Bingxiang He, Youbang Sun, Runze Liu, Che Jiang, Yuchen Fan, Kai Tian, Guoli Jia, Pengfei Li, et al. A survey of reinforcement learning for large reasoning models. *arXiv preprint arXiv:2509.08827*, 2025. 2

[60] Sipeng Zheng, Boshen Xu, and Qin Jin. Open-category human-object interaction pre-training via language modeling framework. In *Proceedings of the IEEE/CVF Conference on Computer Vision and Pattern Recognition (CVPR)*, pages 19392–19402, 2023. 3

[61] Jinguo Zhu, Weiyun Wang, Zhe Chen, Zhaoyang Liu, Shenglong Ye, Lixin Gu, Hao Tian, Yuchen Duan, Weijie Su, Jie Shao, et al. Internvl3: Exploring advanced training and test-time recipes for open-source multimodal models. *arXiv preprint arXiv:2504.10479*, 2025. 1, 3